A Force Identification Method for Slider/Disk Contact Force Measurement

Q. H. Zeng, M. Chapin and D. B. Bogy
Computer Mechanics Laboratory
Department of Mechanical Engineering
University of California at Berkeley, CA 94706

Abstract

Some slider/disk contact exists during operation in almost all current disk drives, and it can result in head crash, wear failure, increased power consumption, and disturbance in the MR read/write signals. In this report, we propose a force identification method to measure the contact force from a single impact. Laser Doppler Vibrometers (LDV) are used to measure the slider's responses. A procedure, which combines experiment and FE analysis, is proposed to model the system, and it is claimed to have many advantages over other methods. The proposed method is successfully applied to measure the contact forces of two nano sliders (a tri-pad and a negative pressure slider) when they make contact with a bump on the disk. A smaller contact force was noted with the negative pressure slider. Also, the contact force is smaller at higher RPM for these two sliders.

I. Introduction

The reliability of the head/disk interface is one of the most important concerns in disk drives. The contacts that may occur in the interface significantly affect the reliability. Contact will occur during the contact-start-stop (CSS) procedure, and it often occurs in the dynamic loading/unloading process. Contact may also occur in the normal operational state because of lower flying heights and surface roughness. Thus, contact exists in almost all current disk drives. These contacts may result in head crash, wear failure, increased power consumption, and disturbance in the MR read/write signals. Therefore, better understanding and control of the contacts are very important in the head/disk interface design.

There are several experimental techniques available to detect whether contact occurs in the interface, and to measure the interactive forces. In our previous report (Zeng and Bogy, 1998), we presented a survey of these techniques. In summary, detection is mainly performed by using transducers such as acoustic emission (AE), piezoelectric (PZT), Laser Doppler Vibrometer (LDV), laser interferometer, electrical resistance, and electrical capacitance. The AE signal and electrical resistance methods are the two best choices for contact detection between the slider and the disk. To better understand and control the contact, we require certain information, such as amplitude and duration, of the forces of the contact. The AE signal (Ganapathi, et al., 1995, and Khurshudov and Talke, 1997), force identification (Matsumoto et al., 1993, Briggs et al., 1991, 1992) and direct measurement (Burger, 1995) have been applied to measure the forces.

The success of these methods has been limited. There is only one paper (Matsumoto et al., 1993) to our knowledge, in which the measured waveforms of the contact force of a 70% slider are presented. Many simulation works on slider/disk contact problems are available. However, the complexity of the problems and lack of experimental data limits the success of the simulation. Therefore, more research work is required on contact force measurement. In this paper, we propose a force identification method to measure the contact force. An LDV is used to measure the slider's responses. A procedure, which combines experiment and FE analysis, is proposed to model the system. The proposed method is successfully applied to measure the contact forces of two (50%) nano sliders (a tri-pad and a negative pressure sliders) when they contact with a bump on the disk. Smaller contact force is noted with the negative pressure slider. Also, the contact force is smaller at higher RPM for these two sliders.

II. A Force Identification Method

2.1 Basic idea and assumptions

Quantitatively measuring the contact forces is much more difficult than detecting whether the contact occurs. Figure 1 illustrates the forces acting on a slider during operation of the disk drive. The position of the contact force action is variable and unknown. By controlling the experimental condition, we can assume that the position is fixed and given, and it is assumed to be at the center of the trailing edge, such as at the small pad of the tri-pad slider. The slider is too small to add any measurement devices on it without alternating the response of the system. Even several very thin wires will obviously affect the properties of the system. Therefore, non-contact measurement is preferred. Due to the

small dimensions of the slider and low amplitude and the wide frequency range of the force, it is too difficult to directly measure the force. Using MEMS technology, Burger (1995) tried to directly measure the force. Supposedly the measurement is of the contact force, but it is actually some kind of response of the slider. Therefore, we apply an indirect measurement method – the force identification method. It is difficult to separate the contact force from the air bearing force, especially in the lower frequency band. We assume that the slider ringing cannot be excited by the air bearings. Then, the force that is obtained based on slider ringing should result from solid contact between the slider and the disk. Thus, we use the slider ringing response to obtain the contact force. Measurement and calibration are very difficult for such small parts with a wide frequency range, and small force. The LDV is well calibrated, accurate in a wide frequency range, and suitable for non-contact measurement. Therefore, we use the LDV to measure the slider ringing.

The basic idea of the force identification method was described in Ewins (1984). There are two steps in the method. The first step that is critical is modeling the system and obtaining the frequency response functions (FRFs) of the system. The second step is measuring responses and calculating the forces. Matsumoto et al. (1993) and Briggs et al. (1991, 1992) used this method to identify the contact forces. They adopted a different approach in the first step, and a similar second step. Matsumoto et al. (1993) used a direct calibration method (breaking pencil lead) to obtain the FRFs of a 70% slider. It is difficult to use this method in current nano (50%) and pico (30%) sliders. Briggs et al. (1992) used the finite element method to model the sliders. The accuracy of the

calculated modal frequencies and lack of the damping parameters limit the application of this method. A small error in the modal frequencies can result in a large error in the identified forces. In this report, we combined the FE analysis results and experimental data to model the system.

2.2 Equations

For linear and self-adjant systems, we have the following relationship:

$$\{X\}_{N_r \times 1} = [H]_{N_r \times N_e} \{F\}_{N_e \times 1} \tag{1}$$

where *{X}* is the Fourier transform of the response vector,

[H] is the frequency response function (FRF)matrix of the system,

{F} is the Fourier transform of the force vector,

N_r is the number of the measured DOFs of the response,

N_e is the number of the forces.

If $N_r > N_e$, and both *[H]* and *{X}* are available, we can obtain the *{F}*

$$\{F\} = \left([H^*]^T [H] \right)^{-1} [H^*]^T \{X\} \tag{2}$$

Performing the inverse Fourier transformation of *{F}*, we can find the time histories of the forces. The key is to obtain *[H]*.

We don't directly measure the FRFs because of the difficulty of applying a measurable excitation force at a specified location, which has energy in an extremely wide frequency range. The FRFs are obtained by using the equation

$$H_{jk}(\omega) = i\omega \sum_{m=1}^{N_m} \frac{\phi_{mj}\phi_{mk}}{G_m\left(\omega^2 - \omega_m^2 + i2\xi_m\omega_m\omega\right)} \tag{3}$$

where f_m, ξ_m, G_m and ϕ_{mj} are the modal frequency ($\omega_m=2\pi f_m$), damping ratio, mode shape and modal mass of mode m. j and k are the DOFs of the response and excitation. It is well known that the modal frequencies can be easily and accurately obtained from expriments but not from calculation. Therefore, the measured modal frequencies will be used in Eq. (3). It is difficult to calculate the damping ratios, but it is easy to obtain them from experiments. Although the measured damping ratios are not as accurate as the frequencies, we still use the measured damping ratios in Eq. (3). The mode shapes can be found by both experiments and FE analysis. For convenience, we use the calculated mode shapes. It is very difficult to accurately measure the modal masses, therefore the calculated modal masses are used in Eq. (3). Because the geometry of the slider is simple, the calculated mode shapes and modal masses should be very accurate if the FE model is verified by experiments. In summary, we use the measured modal frequencies and damping ratios, and the calculated modal masses and mode shapes to synthesize the FRFs by using Eq. (3).

2.3 A procedure to experimentally model the system

We need to obtain the modal frequencies and damping ratios by experiment, which can be identified from the free responses of the sliders. So, the following procedure is proposed.

1) The slider's responses at steady state are measured by the LDV while the slider just contacts the disk without a bump. To prevent the stick/slip problem, a disk with light texture is preferred.

2) The free responses of the slider are obtained by using the random decrement method (Cole, 1973). We use a digital oscilloscope to acquire the slider response data by specifying a suitable trigger level (at about 90% of the maximum response). After averaging in the time domain, we obtain the free responses. Figure 2 a) shows a single shot of the data, and Fig. 2 b) shows the free response obtained after averaging 2000 events.
3) Performing the data preprocessing and parameter identification (Zeng and Bogy, 1999) we can obtain the measured frequencies and damping ratios. The main steps are truncating the free response, adding an exponential window, transforming to the frequency domain, performing curve fitting, and correcting the effects of the window.

III Case Studies

III-1 Experimental System and Materials

The TTI Advanced Tribology Test System with an air bearing spinstand and two Polytec LDVs (single beam 501 and dual-beam 512) were used. The velocity range of 25 mm/s in the frequency band of 0-1500 kHz was selected. A very accurate trigger signal is critical for the experiment because recalled events have to be averaged. From the experiments, we found that the index signal from the spindle motor is not accurate enough to be used in the averaging process in this experiment. Therefore, one LDV was used to measure the bump and trigger the digital oscilloscope (LeCroy 9304c). The laser beam was focused on the disk, near the trailing edge center of the slider. The second LDV was used to measure the slider's responses, first at the trailing edge center and then at the trailing edge-outer rail. An AE sensor was mounted on the suspension holder. The output signal

of the LDV was conditioned with a band-pass filter (Krohn-Hite 3202) from 0.4 MHz to 1.5 MHz. The signals were then acquired with the oscilloscope at a 20 MHz sample frequency for 10000 samples.

Read-Rite 50% tri-pad sliders mounted on HTI 850 suspensions, flying on a super-smooth disk (0.7 nm RMS roughness) with light texture, and a super-smooth disk (0.5 nm RMS roughness) with a bump, were used in the experiments. The bump shape, as shown in Fig. 3, has about 75 nm height. Its shape is almost the same before and after the contact force measurements indicating minimal change in the force excitation through the experiment. For comparison, a negative pressure (NP) slider was also used in the experiments. The air bearing surfaces of the two sliders are shown in Fig. 4. Both sliders have a central pad.

III-2 Modeling

The slider's responses at steady state were measured by the LDV while the slider just contacts the disk (super-smooth disk with light texture and no bump, 8.1m/s, 0 skew). The free responses of the slider were obtained by using the random decrement method (Cole, 1973). Performing the data preprocessing and parameter identification (Zeng and Bogy), we obtained the measured frequencies and damping ratios as shown in Table 1.

The FE models of the two sliders were created by using the ANSYS Finite Element Code. The measured dimensions of the sliders and the material properties (Young's modules =3.93e5. Density =4250 kg/m^3) were used. The model of the tri-pad slider uses

1220 Solid45 elements, and the model of the NP slider uses 540 Solid45 elements. The calculated modal frequencies are shown in Tables 1 and 2, and the mode shapes are shown in Figs. 5 and 6. In the frequency range of 0-1.5 MHz, the tri-pad slider has four modes, and the NP slider has three modes. From Tables 1 and 2, we see that the calculated frequencies are close to the measured frequencies. Therefore, it is believed that the FE models are satisfactory, and the calculated modal masses and mode shapes are accurate.

Next, we used the measured modal frequencies and damping ratios shown in Tables 1 and 2, and the modal masses and shapes shown in Figs. 5 and 6 to obtain the required FRFs, which are shown in Fig. 7. Here, N_r is equal to one, and the force is located at the trailing edge center. N_r is equal to two, and the responses were measured at the center and the out rail of the trailing edge.

III-3 Measured bump responses and identified contact forces

The bump was located at the 39 mm radius under the center of the trailing edge, and the skew angle was set to zero. One LDV measured the bump to trigger the digital oscilloscope while the disk was rotating, another LDV measured the slider's response in the vertical direction, and the AE sensor located at the suspension holder measured the AE signal. The averaging is critical because of the small signal and relatively large noise. Figures 8 and 9 show the measured slider response and AE signal. It is observed that we cannot obtain any meaningful information from the single shot measurements (no average) while the slider flies over the bump. However, we can obtain very good

measurements after the data is averaged. From the LDV measurement (Fig. 8a), we obtained an almost pure impulse response of the second mode of the tri-pad slider.

Using the measured slider responses (Fig. 10) at the center and outer rail of the trailing edge of the tri-pad slider and the FRFs that are shown in Fig. 7a, we can find the contact force by using Eq. 2. The power spectrum and time history of the identified force are also shown in Fig. 10. Similarly, we obtained the bump responses and contact force of the NP slider, which are shown in Fig. 11.

We changed the disk RPM, monitored the sliders' responses, and found that the tri-pad slider can steadily fly and its responses can be measured between 3000 and 8000 disk RPM. However, the bump responses of the NP slider can be measured only between 6000 and 8000 rpm. The contact forces of the two sliders in those rpm ranges were identified. The peak amplitudes and RMS values (from 0 to 0.1 ms) of the bump responses and the forces of the two sliders are shown in Fig. 12. We can see that the NP slider has smaller contact force, and the contact force is smaller at higher RPM. The NP slider has a small central pad from the leading edge to the trailing edge. This feature should decrease the contact force because the flying height increases when the bump passes from the leading edge to the trailing edge. The high RPM increases the flying height and the pitch of the sliders, and thereby decreases the contact force. At the same time, the high RPM increases the contact speed, and thereby increases the contact force. However, the combined effects of the RPM are that the higher the RPM, the smaller the contact force for these two sliders.

From Figs. 10 and 11, it is observed that the identified contact forces have strong oscillations and negative values. It is believed that the causes of this are the measurement noise and the effects of the band pass filters that are applied in the measured responses and the identified forces. Figure 13 shows the effects of the filter. Assuming the contact force is a half-harmonic function with a 5 mN amplitude and 1.5 μs duration, we obtained a strong oscillation in the simulated contact force after the filter. Therefore, the band pass filter significantly affects the force identification.

IV. Conclusion

a) A force identification method is proposed to obtain the solid interactive forces between disks and sliders. The method is successfully applied to measure the contact forces of two nano sliders when they contact a bump on the disk.

b) It is found that more reliable data can be measured by using the LDV than the AE sensors. Therefore, the LDV was used to measure the slider's responses. A precision trigger and averaging method are necessary for accurate measurement.

c) Modeling the system is critical for force identification. A procedure, which combines experiment and FE analysis, is proposed. The procedure has many advantages over other methods. For example, there is no modification of the system. The status of the system in the modeling stage is almost identical to the status in the stage of the force

identification. It is more accurate than the methods in which only analytic data is used. It is more convenient than the direct calibration methods.

d) The forces due to contact of two different sliders with a bump on the disk are measured at various spindle speeds. Smaller contact force is noted with the negative pressure slider. Also, the contact force is smaller at higher RPM for these two sliders.

e) The biggest challenge in the force measurement is how to separate the air bearing force and the solid interactive forces in a lower frequency band. Moreover, it is still very difficult to use the proposed method to obtain the contact forces of the smaller sliders (i.e., 30% pico slider) because of the sensitivity limitation of the LDV.

Acknowledgments

This work is supported by the Computer Mechanics Laboratory (CML), University of California at Berkeley, and the National Storage Industry Consortium (NSIC) through its EHDR program.

References

Briggs,J. C., 1991, “Force Identification using Extracted Modal Parameters, with Application to Glide Height Testing of Computer Hard Disks,” Ph.D thesis, MIT.

Briggs, J. C., Chang, M. K. and Tse, M. K., 1992, “High Frequency Slider Vibrations During Asperity Impacts in Rigid Magnetic Disk Systems,” *ASME, Adv. Info. Storage Syst*., V. 4 pp. 181-194.

Burger, G. J., 1995, “A Slider Motion Monitoring System - Measuring Contact and Friction Froces in Rigid Disk Storage Devices,” *Thesis, Dept. of Applied Physics*, Univ. of Twente, Netherlands.

Cole, H.A. Jr., 1973, “On-line failure detection and damping measurement of Aerospace structure by random decrement signature,” NASA CR-2205.

Ewins, D. J., 1984, “Modal Testing: Theory, Practice and Application,” Research Studies Press, pp. 246-251.

Ganapathi, S.K., Donovan, M. and Hsia, Y.T., 1995, “Contact Force Measurement at the Head/Disk Interface for Contact Recording Heads in Magnetic Recording,” Proc. Of SPIE Vol 2604 – The intl. Society for Optical Eng., Philadelphia, Penn., Oct. 23-24, pp. 236-243.

Khurshudov A.G. and Talke, F. E., 1997, “Investigation of Proximity Recording Sliders Using Acoustic Emission,”, Proc. Of Intl. Conf. On Micromechantronics for information and Precision Equipment, Tokyo, July, 20-23, pp. 439-442.

Matsumoto, M., Iida, A. and Hamaguchi, T., 1993, “Measurement of Slider/Disk Collision Forces Using Acoustic Emission Source Wave Analysis,” *ASME, Tribology Trans.*, Vol. 36(4), pp. 736-740.

Zeng, Q. H. and Bogy, D. B., 1998, “A Survey on Detection and Measurement of the Interaction between Disk and Slider,” Technical Report No. 98-002, Computer Mechanics Lab, Dept. of Mechanical Engineering, UC-Berkeley.

Zeng, Q. H. and Bogy, D. B., 1999, “Experimental Evaluation of Stiffness and Damping of Slider-Air Bearings in Hard Disk Drives,” *ASME J. of Trib.*, Vol. 121(1), 102-107.

Table 1 Modal frequencies and damping ratios of the tri-pad slider

No	Calculated Frequencies (kHz)	Measured Frequencies (kHz)	Measured Damping Ratios(%)
1	624.00	665.86	0.300
2	824.5	808.48	0.223
3	1142.5	1187.4	0.321
4	1477.1	1464.2	0.192

Table 2 Modal frequencies and damping ratios of the NP slider

No	Calculated Frequencies (kHz)	Measured Frequencies (kHz)	Measured Damping Ratios(%)
1	706.6	712.71	0.154
2	908.5	907.04	0.524
3	1433.2	1403.2	0.117

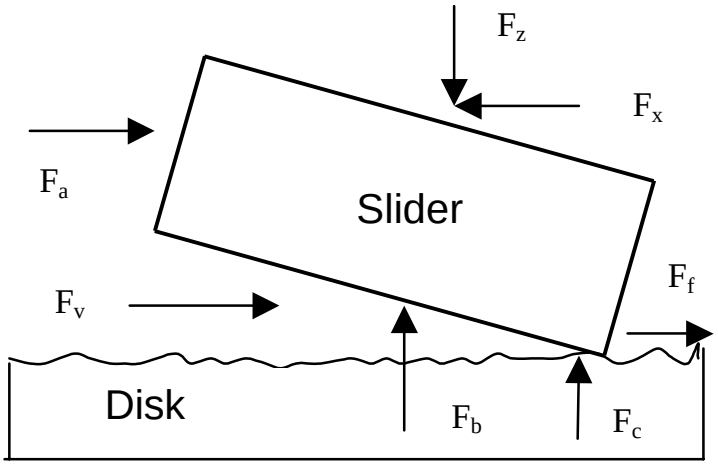

F_a Aerodynamic drag
F_b Air bearing force
F_c Contact force
F_f Friction force
F_v Viscous shear force
F_x Suspension load in X direction
F_z Suspension load in Z direction

Fig. 1 The forces acting on the slider

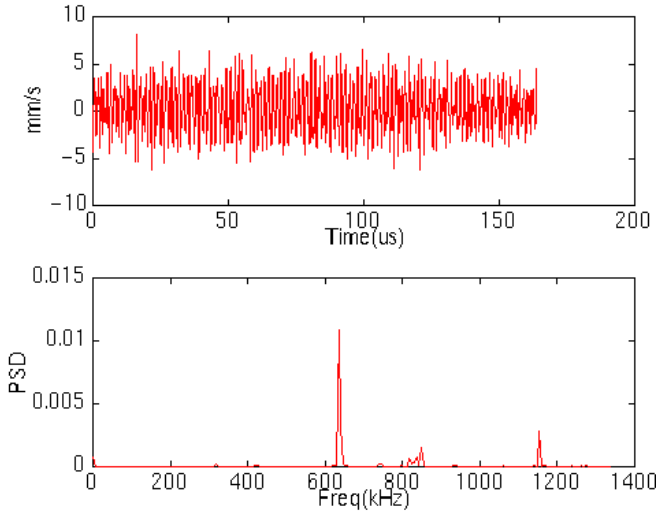

a) Measure the slider responses at the steady state (9.2m/s, 0 skew, the slider just contacts the disk)

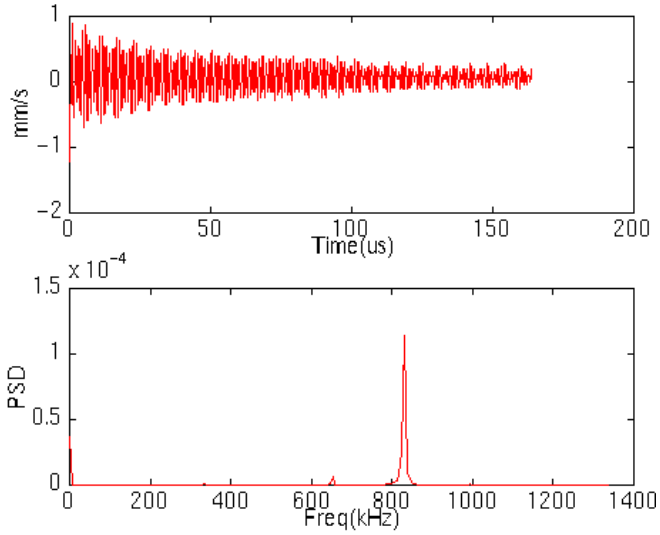

b) The free responses of the slider obtained by using the random decrement method.

Fig. 2 Measured slider response for identifying the modal frequencies and damping ratios of the system

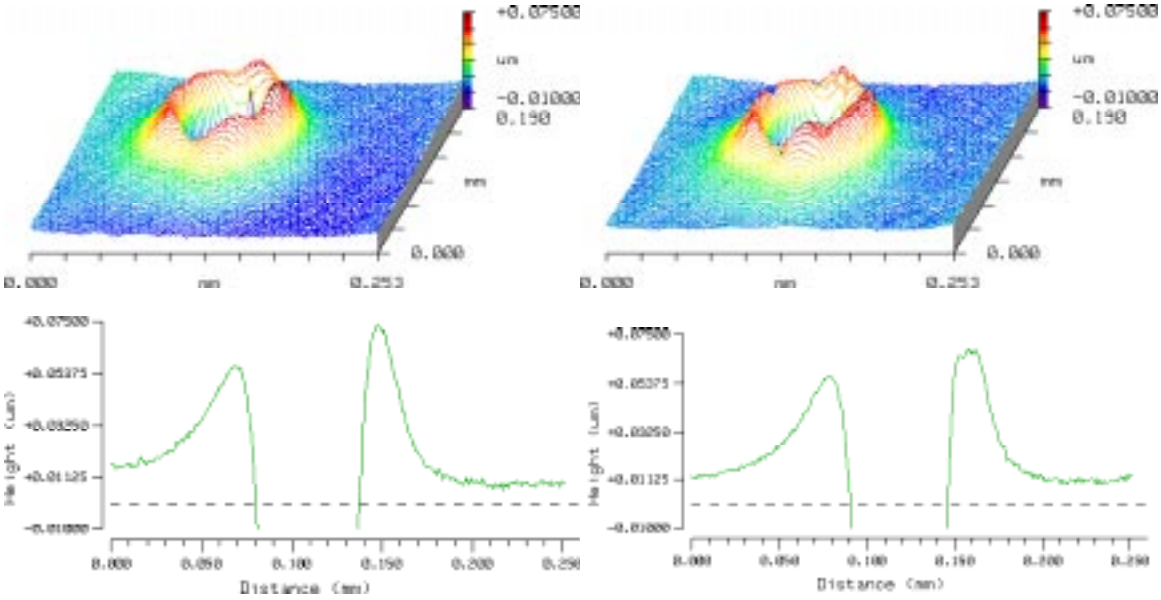

a) Before the contact force measurement b) After the measurement

Fig. 3 Bump shape

a) Tri-pad slider b) Negative pressure (NP) slider

Fig. 4 Air bearing surfaces of the two sliders

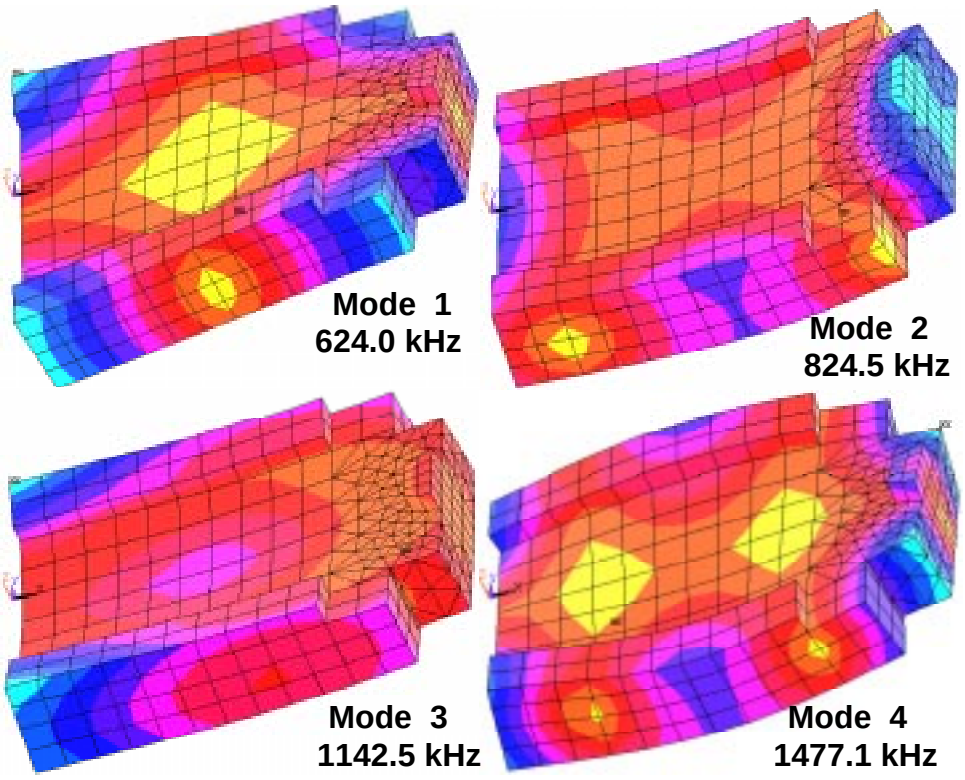

Fig. 5 Mode shapes of the tri-pad slider

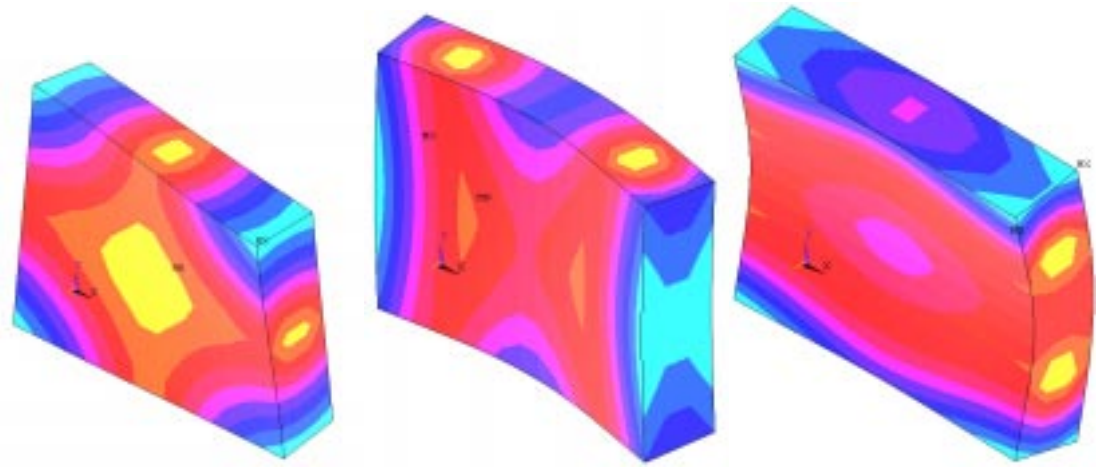

a)Mode 1 (706.6 kHz) b) Mode 2 (908.5 kHz) c) Mode 3 (1433.2 kHz)

Fig. 6 Mode shapes of the NP slider

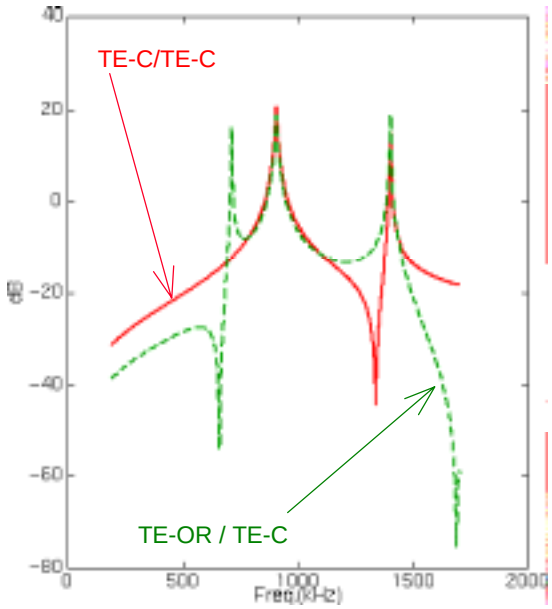

a) The tri-pad slider

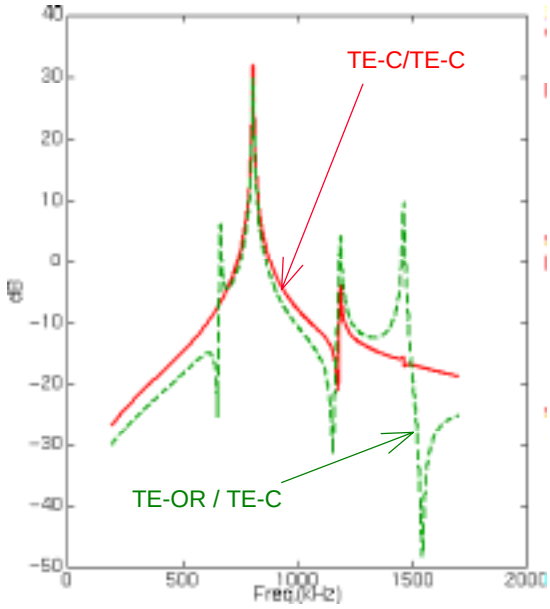

b) The NP slider

Fig. 7 FRFs of the two sliders - excited at trailing edge center (TE-C), responsed at trailing center and outer rail (TE-OR)

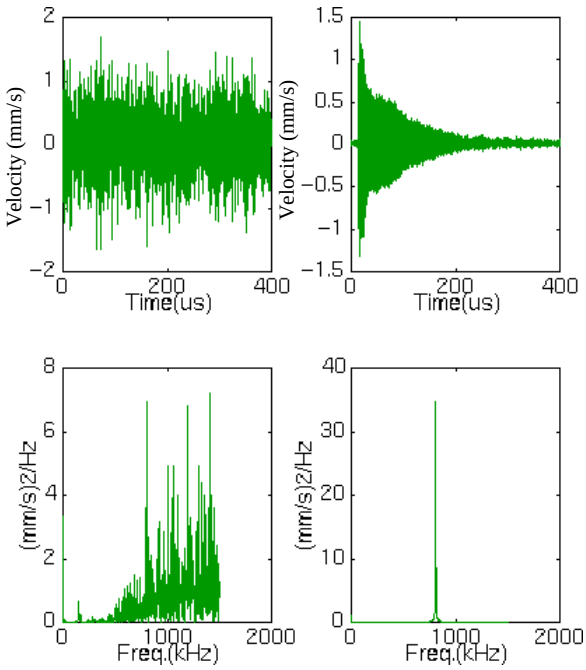

a) single shot b) 2000 average

Fig.8 Measured responses at the trailing edge center of the tri-pad slider hitting the bump at 6000 RPM

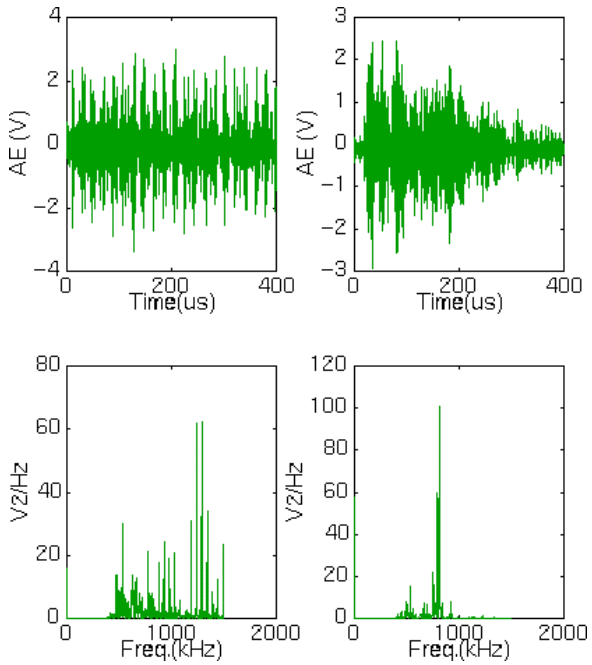

a) single shot b) 2000 average

Fig.9 Measured AE signals of the tri-pad slider hitting the bump at 6000 RPM

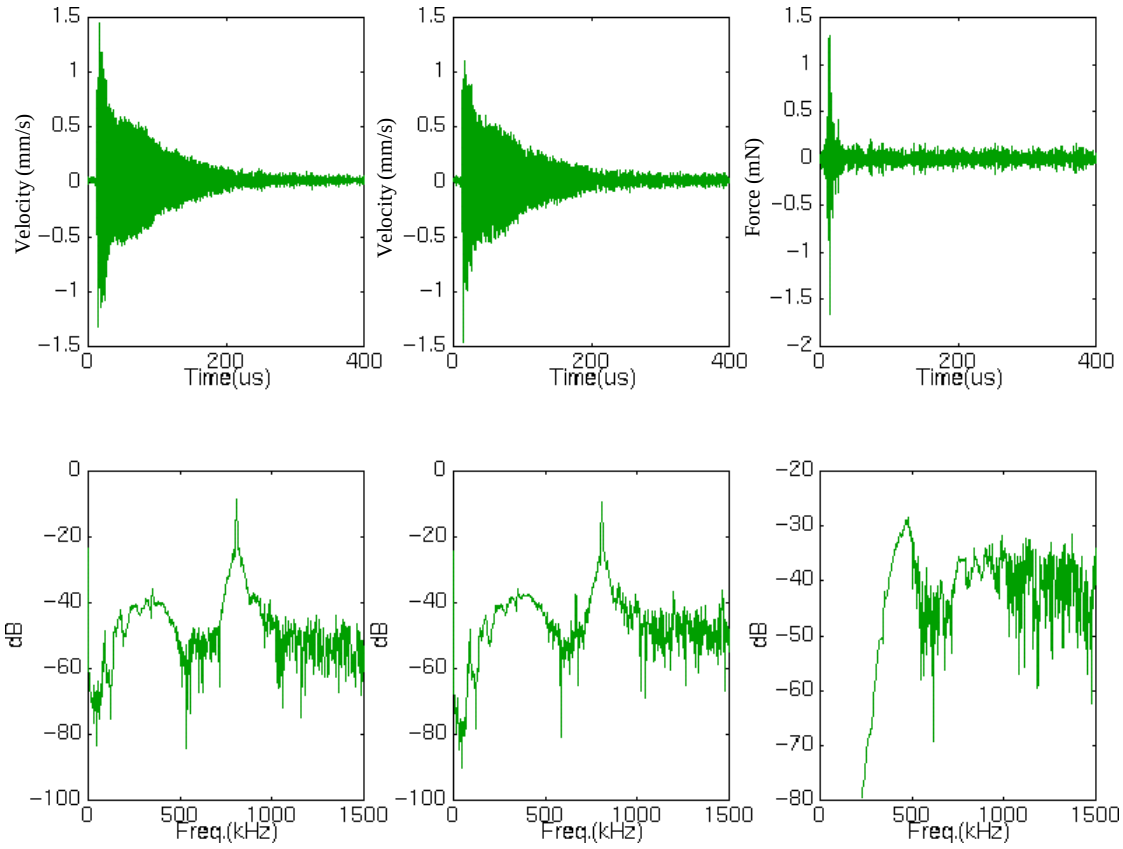

a) at the trailing edge center b) at trailing edge outer rail c) Identified contact force

Fig. 10 Measured responses and identified contact force of the tri-pad slider at 6000 RPM

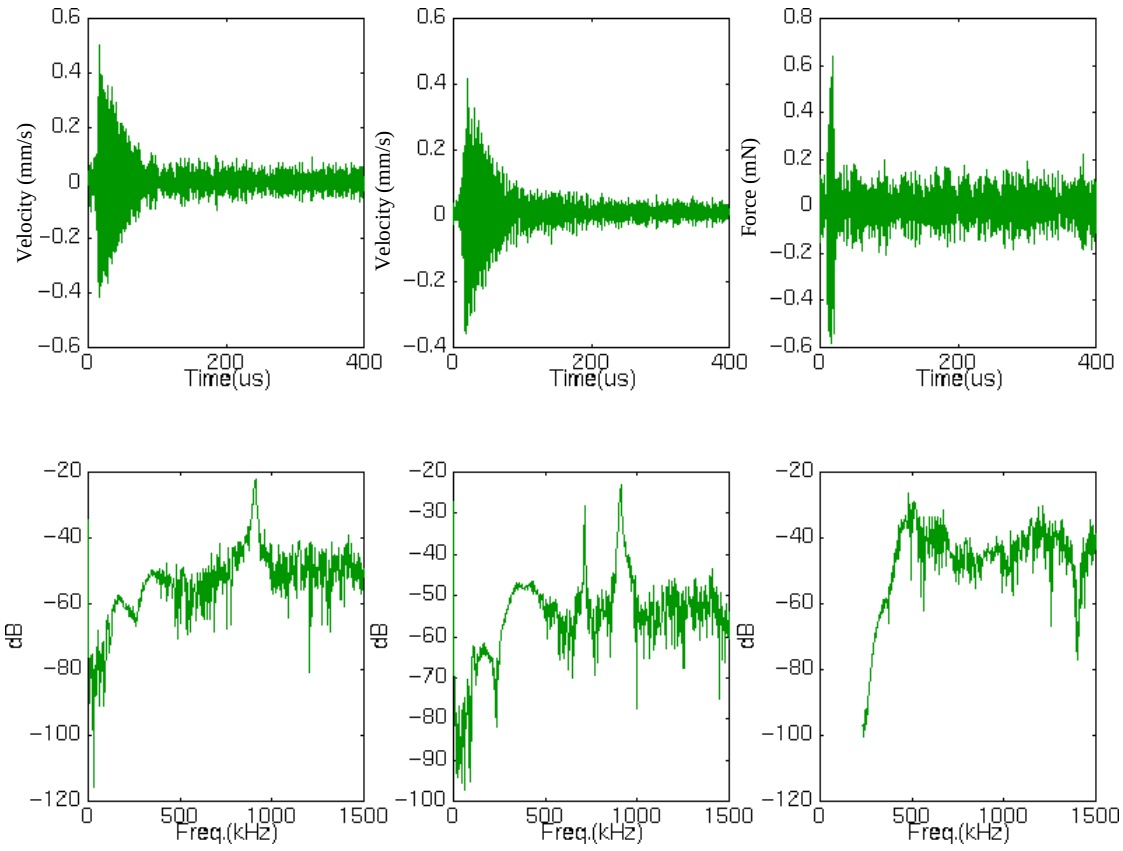

a) at the trailing edge center b) at trailing edge outer rail c) Identified contact force

Fig. 11 Measured responses and identified contact force of the NP slider at 6000 RPM

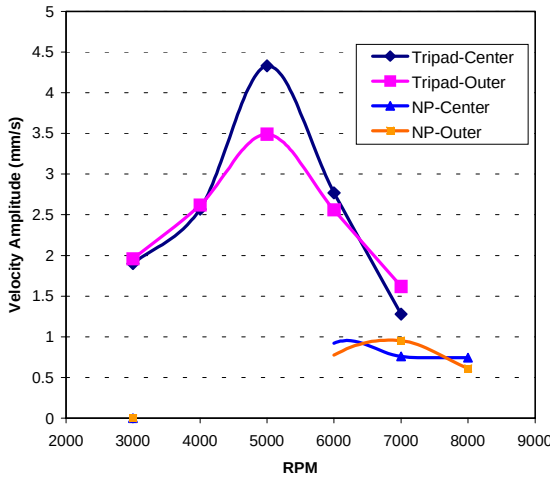

a) Sliders' response via disk RPM

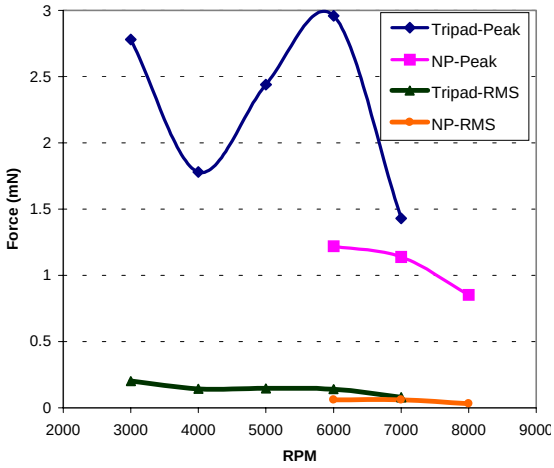

b) Identified contact forces

Fig. 12 Sliders' response and contact forces via disk RPM

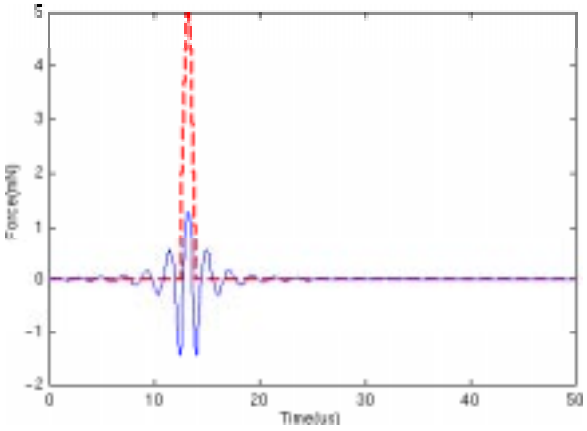

Fig. 13 The effects of the 0.4-1.5 MHz band pass filter – simulation (dot line is original force; solid line is one after the filter)